J. Fluid Mech. (2002), *vol.* 459, *pp.* 429–443. © 2002 Cambridge University Press
DOI: 10.1017/S002211200200811X Printed in the United Kingdom

The integral scale in homogeneous isotropic turbulence

By HONGLU WANG[1] AND WILLIAM K. GEORGE[2]

[1]Belcan Corporation, Automated Analysis Division, Novi, MI 48375, USA

[2]Chalmers University of Technology, SE-412 96 Göteborg, Sweden

(Received 8 January 2001 and in revised form 3 December 2001)

A simple spectral model is used to examine what is required to determine the energy and integral scale in homogeneous isotropic turbulence. The problem is that these are determined in part by the largest scales of the turbulence which are either not simulated at all by DNS or experiments, or cannot be estimated because of an insufficient statistical sample. The absence of scales an order of magnitude below the peak in the energy spectrum is shown to affect the determination significantly. Since this energy peak shifts to lower wavenumbers as the flow evolves, the problem becomes progressively worse during decay. It is suggested that almost all reported integral scales for isotropic decaying turbulence are questionable, and that the power laws fitted to them are seriously in error. Approximate correction using the spectral model shows that recent DNS data which decay as $u^2 \propto t^n$ with constant n, are also consistent with $L \propto t^{1/2}$.

1. Introduction

There have been numerous attempts over the past four decades to determine the integral scales of isotropic decaying turbulence, both from experiment and more recently using DNS. Of particular interest has been how the integral scale varies with time during decay. Most use a power law variation, $L \propto t^m$ with values of m ranging from $\frac{2}{7}$ (Kolmogorov 1941) to $\frac{1}{2}$ (Dryden 1943). The latter value is of some special interest since it was originally derived by Dryden from an extension of the von Kármán & Howarth (1938) similarity hypothesis, and subsequently from a more general equilibrium similarity theory by George (1992). In fact, both of these approaches concluded that the integral scale and Taylor microscale, λ, should remain in constant ratio throughout decay. George (1992) showed that the experimental longitudinal and lateral integral scales obtained by Comte-Bellot & Corrsin (1971) appeared to confirm this. By contrast, Wang *et al.* (2000) observed that the ratio of L/λ continued to drop slowly for the DNS data of Wray (1998), a matter of considerable concern for them, since the equilibrium similarity theory accounted for numerous other features of the data.

Comte-Bellot & Corrsin (1966) summarized the variation of integral scale with time for a number of experiments. The data were fitted by powers in time with exponents ranging from 0.30 to 0.53. It is commonly believed (e.g. Lohse 1994) that 0.4 was the preferred choice of these authors, but a careful reading of their manuscript makes it clear that they were extremely skeptical of all values because of the limited number of data points. Nevertheless, it has become more or less universal because it is in

https://doi.org/10.1017/S002211200200811X Published online by Cambridge University Press

approximate agreement with the infinite Reynolds number idea that $L \propto u^3/\epsilon$ if $u^2 \propto t^{-1.25}$, as is also commonly believed (Batchelor 1953; Sreenivasan 1984).

In fact, experiments and DNS routinely produce values of the energy decay exponent n which are quite different from $n = -1.25$. Moreover, the cited value of Comte-Bellot & Corrsin (1966) for the integral scale variation of $m = 0.4$ appears to have been chosen only because it agreed well with the correlation discard simulations of Deissler (1961) (and about which they also expressed reservations). Comte-Bellot & Corrsin (1971) expressed even more reservations about the integral scales, both because of their concern that tunnel size limitations affected the large scales, and because of problems presented by its determination. In particular, they used a parabolic fit to the one-dimensional spectra at low wavenumbers, but expressed concern that their spectra may not have been measured to low enough wavenumbers for the parabolic approximation to be valid (see their appendices).

The DNS data would appear, on the surface at least, to be able to settle at least some of these questions. DNS computes *periodic turbulence*, so the results are at best only an approximation to isotropic turbulence for wavenumbers above the lowest wavenumber in the simulation. As noted by de Bruyn Kops & Riley (1998) and Wang *et al.* (2000), there are reasons to suspect that there is a problem if the peak in the energy spectrum is at wavenumbers not sufficiently greater than the lowest wavenumber. Even when this does not seriously affect the overall energetics or integral scales early in the calculation, there is reason for concern about the later times since the scales grow with time. However, in addition to concern about the actual energetics, there is also concern about information which is not available owing to averaging limitations. The simulations of decaying turbulence provide useful information about averaged quantities only for scales sufficiently smaller than the computational domain where spatial averages can be used to approximate ensemble averages. Thus, the estimate of integral scales from the spectrum, for example, can be severely reduced by the unavailability of the lowest wavenumbers which may contribute most to it.

This paper uses a simple spectral model to examine the effect of missing large scales (or low wavenumbers) on the determination of the integral scale (and energy as well). The model will allow a quantitative evaluation of how the 'measured' integral scale deviates from the 'true' integral scale that would have been obtained had all the necessary low wavenumbers been present or accurately simulated. The model will be used to approximately correct two recent DNS attempts to simulate decaying homogeneous turbulence.

2. The fundamental equations and the spectral models

In the analysis presented herein, semi-empirical forms of the three-dimensional energy spectrum function, $E(k,t)$ will be considered. $E(k,t)$ is the integral over spherical shells of radius k of the trace of the three-dimensional spectrum, which is itself the three-dimensional Fourier transform of the two-point velocity spectrum tensor (Batchelor 1953). The theory of isotropic turbulence assumes an infinite domain, hence the $E(k,t)$ to which this theory strictly applies must be defined over all wavenumbers. Thus, any attempts to realize such flows are, at best, approximations. This is, of course, well-known, yet there is only limited understanding of the consequences. As a result, theoretical results are called into question because they differ from the experiments, even though the experimental results might have been anticipated. The approach used here is to assume the theory for an infinite domain (as detailed below)

https://doi.org/10.1017/S002211200200811X Published online by Cambridge University Press

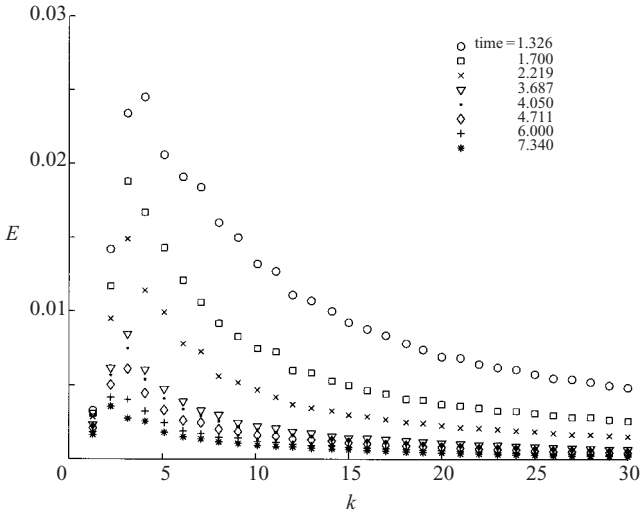


FIGURE 1. $E(k)$ versus k for the Wray (1998) DNS data.

to be correct, then show that the measurements can be accounted for by considering the contribution of the largest scales which the experiments and simulations cannot produce.

Of primary interest here will be the kinetic energy, $\frac{1}{2}\langle u_i u_i \rangle \equiv \frac{3}{2}u^2$, and the integral scale, L. For homogeneous, isotropic turbulence, these are related to $E(k,t)$ by (Batchelor 1953):

$$\tfrac{3}{2}u^2 = \int_0^\infty E(k,t)\mathrm{d}k, \tag{2.1}$$

and

$$L = \frac{\pi}{2u^2}\int_0^\infty \frac{E(k,t)}{k}\mathrm{d}k. \tag{2.2}$$

It is clear from equation (2.2) that the integral scale determination is more heavily weighted by the lowest wavenumbers. This is the source of the problems addressed by this paper.

The problem posed by the missing wavenumbers is clearly evident in figures 1 and 2 which show plots of $E(k)$ and $E(k)/k$ versus k of the DNS data of Wray (1998) for various times during decay. Although for small times, there are several spectral estimates below the peak in $E(k)$, by the end there is only one. For DNS of decaying turbulence, the spectrum is obtained by 'averaging' the modulus squared of the Fourier coefficients over finite-thickness shells between $k - \Delta k/2$ and $k + \Delta k/2$ (instead of the more familiar ensemble averaging or time averaging of a stationary experiment). This presents a special problem at lowest wavenumber, both because of the very few Fourier coefficients available and the fact that the spectrum is changing most rapidly there. The problem can be easily avoided by moving the spectral peak to much higher wavenumbers, but this means the simulations will be at proportionally lower Reynolds numbers. So most opt for the highest Reynolds number possible by squeezing the low end, since it is presumed the highest wavenumbers are of the most interest. Only recently has what is happening at the lowest wavenumbers been of major concern (e.g. Wang *et al.* 2000)

https://doi.org/10.1017/S002211200200811X Published online by Cambridge University Press

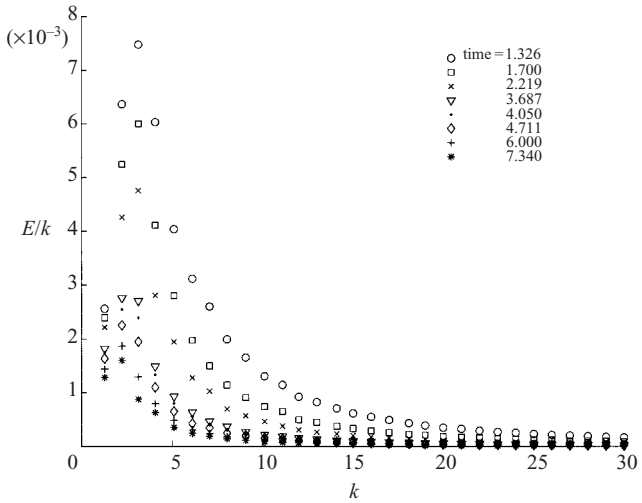


FIGURE 2. $E(k)/k$ versus k for the Wray (1998) DNS data.

3. The importance of the missing low wavenumbers

As noted above, in the real world of experiments and computer simulations, wavenumbers below a certain value, say k_L, are not available because the scales are larger than the size of the facility or computational domain, or simply because they have not been measured or computed because of other limitations (like instrument response or averaging). Whatever the cause, without arbitrary interpolation the portion of the energy that can be determined from the realized spectrum, say $\frac{3}{2}u_m^2$, is only:

$$\tfrac{3}{2}u_m^2 \equiv \int_{k_L}^{\infty} E(k,t)\mathrm{d}k. \tag{3.1}$$

Similarly, the most that can actually be computed from the data is the 'measured' integral scale, L_m defined by the partial integral:

$$L_m \equiv \frac{\pi}{2u_m^2}\int_{k_L}^{\infty}\frac{E(k,t)}{k}\mathrm{d}k. \tag{3.2}$$

To proceed further requires a knowledge of the spectrum, $E(k)$. In general, $E(k,t)$ increases from zero at zero wavenumber as some power of k; peaks somewhere near the inverse of the integral scale, say k_p; then rolls-off approximately as $k^{-5/3}$ through an inertial subrange; and finally, rolls-off exponentially in the dissipative range. Also, as the energy decays, the spectral peak shifts to lower and lower wavenumbers and the overall spectral levels diminish (see figure 1). For the purposes of this paper, neither the exponential roll-off in the dissipative range nor the deviations from the $k^{-5/3}$ roll-off are important.

The simplest model containing the essential features is a generalization of the model spectrum originally proposed by von Kármán & Howarth (1938). In non-dimensional form using u^2 and L it is given by:

$$E(k,t) = u^2 L\frac{C_p(kL)^p}{[1+(k/k_e)^2]^{p/2+5/6}}. \tag{3.3}$$

https://doi.org/10.1017/S002211200200811X Published online by Cambridge University Press

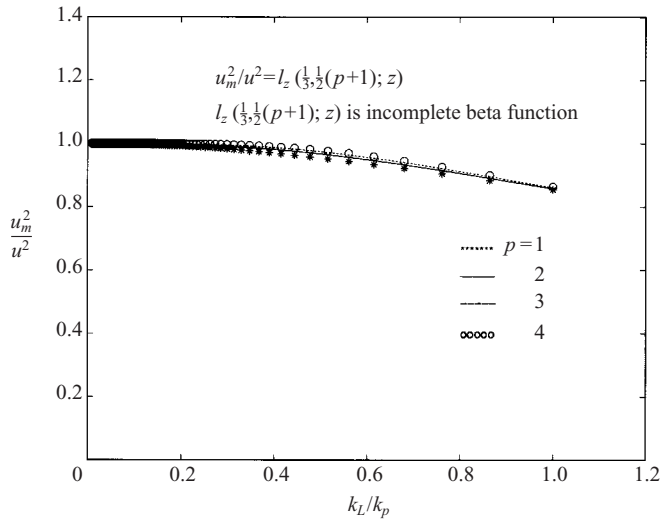


FIGURE 3. Ratio of energy above k_L to total energy versus k_L/k_p.

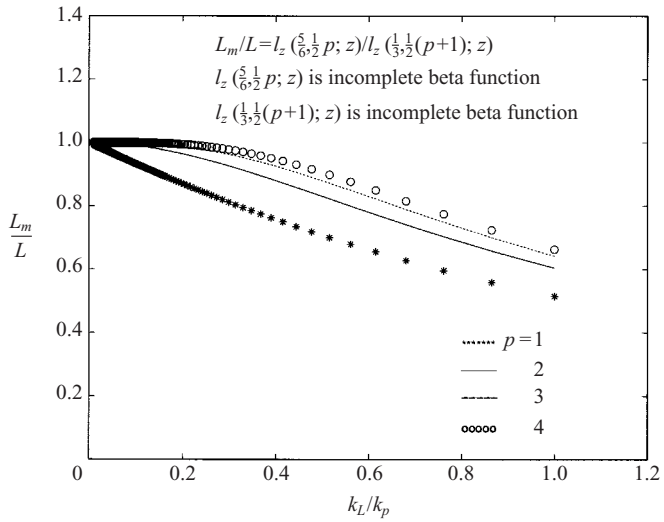


FIGURE 4. Ratio of portion of integral scale above k_L to total integral scale versus k_L/k_p.

This particular spectrum is the infinite Reynolds number limit of the spectrum recently created by Gamard & George (2000) using near asymptotics to fit the extensive grid turbulence spectra of Mydlarski & Warhaft (1996), and is identical to it for the low wavenumbers of primary interest here. The coefficients C_p and k_e (or equivalently L) are interrelated and can be uniquely determined as a function of p by substitution into equations (2.1) and (2.2). The details and results are summarized in Appendix A. The primary advantage of this spectrum is that it leads to the analytical solutions derived below for the missing wavenumbers.

Figures 3 and 4 show plots of u_m^2/u^2 and L_m/L as functions of k_L/k_p where k_L is the lowest available wavenumber and k_p is the wavenumber at which the energy spectrum peaks. The ratios were computed by substituting equation (3.3) into equations (2.1), (2.2), (3.1) and (3.2). The details of this computation are in Appendix B, but the

https://doi.org/10.1017/S002211200200811X Published online by Cambridge University Press

results are simple and given by:

$$\frac{u_m^2}{u^2} = I_z\left(\tfrac{1}{3}, \tfrac{1}{2}(p+1); z\right), \tag{3.4}$$

$$\frac{L_m}{L} = \frac{u^2}{u_m^2} I_z(\tfrac{5}{6}, \tfrac{1}{2}p; z) = \frac{I_z(\tfrac{5}{6}, \tfrac{1}{2}p; z)}{I_z(\tfrac{1}{3}, \tfrac{1}{2}(p+1); z)}, \tag{3.5}$$

where I_z is the incomplete beta function and the variable z is defined by:

$$z \equiv \frac{1}{[1 + (3p/5)(k_L/k_p)^2]}. \tag{3.6}$$

It can be seen from the plots that energy ratio is relatively insensitive to the value of p, the exponent of the spectrum near $k = 0$. It is also obvious from figure 3 and the equations above why it is possible to obtain the overall energetics of the decay to within a few per cent even for values of $k_L/k_p = 0.5$, which is not uncommon near the end of DNS attempts to simulate decaying homogeneous turbulence (e.g. Wray 1998). Even at this late stage in the calculations, the missing wavenumbers contribute less than 10% to the total energy, and have only a tiny effect on the decay rate (which is proportional to the integral of k^2E, and hence barely sensitive at all). By considering the flux of energy to the low wavenumbers and requiring it be negligible, de Bruyn Kops & Riley (1998) suggest that k_L/k_p should be less than 0.3. This appears from figure 3 to be approximately correct, but clearly this ratio must be maintained throughout the simulation to estimate the energy decay rate properly. It is important to note, however, that even the progressive loss of a few per cent of the energy can make an important difference in the apparent power law exponent of the decay, especially if the decay exponent is to be determined to two decimal places as is customary. This loss can make the power law exponent appear to be time-dependent even if it is not.

The integral scale ratio shown in figure 4, by contrast, is very sensitive to the low-wavenumber behaviour, so the choice of p is crucial in evaluating the errors. For example, for $p = 2$, the integral scale computed from the spectral data above k_L is more than 40 % low for the same $k_L/k_p = 0.5$ used above for the energy. These missing wavenumbers have an effect on the apparent temporal variation which is not small, and lead to significant underestimates of the growth rate exponent, m, or make it appear to be time-dependent.

4. Correcting the integrated spectra for the missing wavenumbers

A significant advantage of these analytical results is that they can be used to estimate what the proper values of u^2 and L might have been had the missing low wavenumbers been available. This is only obvious when the variable z defined by equation (3.6) is expressed in terms of the true integral scale L. In Appendix A it is shown that:

$$k_pL = \frac{3\pi}{4}\left[\frac{3p}{5}\right]^{1/2} \frac{B(\tfrac{5}{6}, \tfrac{1}{2}p)}{B(\tfrac{1}{3}, \tfrac{1}{2}(p+1))}, \tag{4.1}$$

so the conversion from k_L/k_p to k_LL is trivial. It is always assumed that k_L is known.

Obviously, correction is not simple because the true integral scale, L, appears on both sides of equation (3.5). This implicit relation can be solved, however, by

https://doi.org/10.1017/S002211200200811X Published online by Cambridge University Press

straightforward iteration: simply supply the values for u_m^2 and L_m along with the cutoff wavenumber, k_L, and iterate the choices of u^2 and L until equations (3.4) and (3.5) are satisfied. The only problem is how to choose p without biasing the answer. As should be clear from the spectral plots above, it is not possible to make this choice by fitting the spectral data since there are no estimates to fit. The results of an alternative procedure will be presented below, along with discussion of the validity of the entire procedure.

Such a correction procedure makes sense only if the part of the spectrum that is available from the data itself reasonably models a homogeneous turbulence. This subject was recently considered in detail by George *et al.* (2001), the considerations of which apply here. The approach used there was first to show that the data under consideration are consistent with a homogeneous turbulence undergoing a power law decay (i.e. $u^2 \propto t^n$) with constant power law exponent, n. Then the spectral exponent p was determined from the similarity relation of George (1992), i.e.

$$p = -2n - 1. \tag{4.2}$$

Finally, the choices and corrections made are shown to be consistent with the kinematical and dynamical constraints of decaying isotropic homogeneous turbulence.

If the turbulence is decaying as $u \propto t^n$ with constant n, then it is easy to show from the definitions that the Taylor microscale squared must grow linearly (Batchelor 1953), i.e.

$$\lambda^2 = 2Av(t - t_o), \tag{4.3}$$

where t_o is a virtual origin. Moreover, the coefficient can easily be shown to be determined entirely by the decay exponent to be exactly:

$$A = -\frac{5}{n}. \tag{4.4}$$

The entire question of the virtual origin can be postponed by considering the derivative of equation (4.3) which reduces to:

$$\frac{1}{v}\frac{\mathrm{d}\lambda^2}{\mathrm{d}t} = -\frac{10}{n}. \tag{4.5}$$

Thus, if the turbulence is decaying as a power law in time with constant exponent, n, a plot of $\mathrm{d}\lambda^2/\mathrm{d}t$ versus time shows a flat region, and its level yields unambiguously the power law decay exponent, n.

Figures 5(a) and 5(b) show plots of the corrected and uncorrected values of $\mathrm{d}\lambda^2/v\mathrm{d}t$ for the DNS data sets of Wray (1998) shown earlier and the de Bruyn Kops & Riley (1998) data. Both are 512^3 simulations. For the Wray data, after a long transient there is at most a small region ($5.0 < t < 6.3$) where the exponent can be reasonably assumed constant, before it tails off slowly. (However, even for this limited 'flat' region the value drops from 6.7 to 6.5.) The de Bruyn Kops & Riley data, by contrast, settle quickly into an extensive region ($0.4 < t < 0.7$) which is nearly flat (for the corrected data to within one per cent). The roll-off for large times of the uncorrected data is compensated for by the correction for both data sets (perhaps a bit too much for the very late times of the de Bruyn Kops & Riley data), suggesting that both are better approximations to an $n = constant$ decay than was immediately apparent from the original data.

The corrected data was computed by solving equations (3.4) and (3.5) above for each time step using the values of u_m^2 and L_m determined by integrating the DNS spectra from and above k_L using a trapezoidal rule. A new value of decay rate and λ^2

https://doi.org/10.1017/S002211200200811X Published online by Cambridge University Press

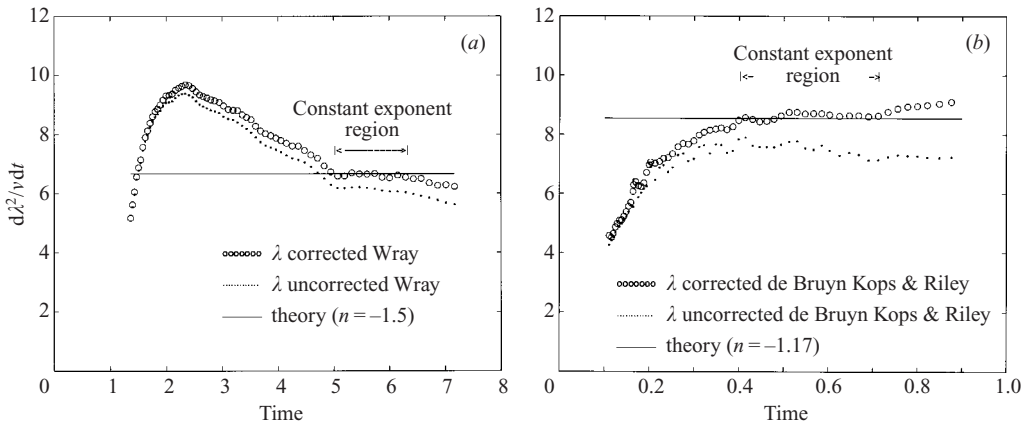


FIGURE 5. Corrected and uncorrected $d\lambda^2/\nu dt$ versus t for (a) Wray (1998) DNS data, (b) de Bruyn Kops & Riley (1998) DNS data.

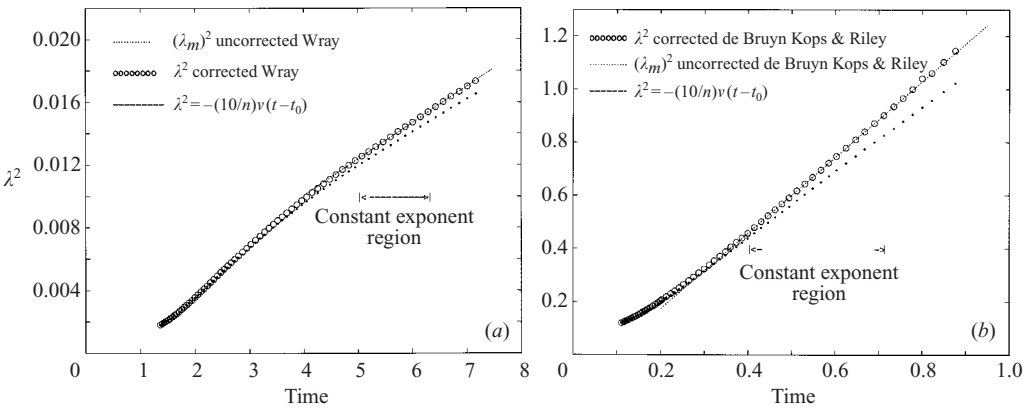


FIGURE 6. Corrected and uncorrected λ^2 versus t for (a) Wray (1998) DNS data, (b) de Bruyn Kops & Riley (1998) DNS data.

was then computed from the new u^2. This process was continued until the assumed value of p was consistent with equations (4.5) and (4.2). Unlike the usual curve-fitting where almost any choice of exponent can be made to work (usually by choosing a virtual origin), this process was quite sensitive and there was virtually no latitude for arbitrary choices. The processs required numerous iterations to achieve accuracy to the second decimal place in n (or p). The uncorrected values were $n = -1.3$ and -1.6 for the de Bruyn Kops & Riley and Wray data, respectively. The final values for the corrected data were $n = -1.17$ (de Bruyn Kops & Riley) and -1.5 (Wray), which correspond to $p = 1.34$ and $p = 2$, respectively.

Figures 6(a) and 6(b) show the variation of the Taylor microscale squared for both data sets before and after correction. The virtual origin has been chosen for the best linear fit to the constant power exponent region, $t_o = -0.35$ for Wray and $+0.078$ for de Bruyn Kops & Riley. The coefficient given by equation (4.4) provides the slope. These choices are nearly perfect for both data sets, fitting the de Bruyn Kops & Riley data over the constant power law range to within 0.06%, and the Wray data to within 0.01%.

Plots of the corrected and uncorrected energy look almost identical to each other,

https://doi.org/10.1017/S002211200200811X Published online by Cambridge University Press

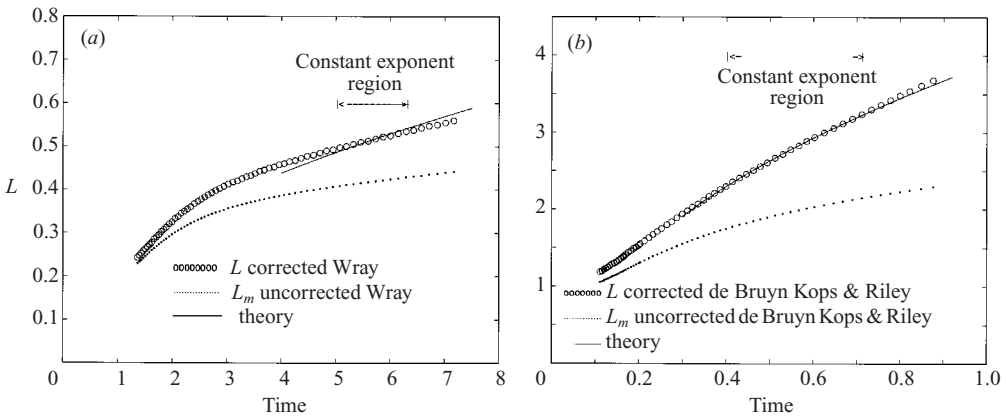


FIGURE 7. Corrected and uncorrected L versus t for (a) Wray (1998) DNS data, (b) de Bruyn Kops & Riley (1998) data.

so are not shown. The power law with constant n fits the Wray and de Bruyn Kops & Riley data to within 0.2% and 0.3%, respectively, for the time ranges identified above using the same virtual origins. It should be noted that the corrected values of u^2 are not significantly different from what would have been obtained by a simple interpolation of the energy spectrum to zero (as is often done), since the error is not very sensitive to p. Such a simple interpolation is not reasonable for the integral scale, however, since the low-wavenumber contribution is strongly dependent on the assumed value of p, hence this iterative procedure.

Figures 7(a) and 7(b) show the variation of the corrected and uncorrected integral scale with time for both sets of data. By comparison to the corrections to the energy and Taylor microscale which were quite small, the integral scale differences are large, especially for the longest times. The reasons for this, of course, are obvious from the spectral plots (shown in dimensionless form in Appendix A), since there are few data for wavenumbers below the spectral peak. Also shown on each plot is a line showing a square root variation with time using the virtual origin determined from the Taylor microscale above. The fit to the de Bruyn Kops & Riley data over the region where the exponent is constant is to within 0.2%, and thus consistent with the George (1992) prediction. The square root line is less satisfactory for the Wray data for which the variation is about 1% over even the very limited approximately constant exponent range. The reason for the difference is not clear, but is perhaps attributable to the fact that there is really no range where $\mathrm{d}\lambda^2/\nu\mathrm{d}t$ is constant for this data set, even when corrected.

Figures 8(a) and 8(b) show the variation of L/λ with time for the two sets of data. The value of L/λ is 3.4 for the corrected de Bruyn Kops & Riley data to within 0.1% over the constant power region. However, the same ratio is also nearly constant (to within 0.4 %) for the entire range of the data. The Wray data, by contrast, drops from 4.45 to 4.31 over the region $5 < t < 6.3$. Even so, the relative drop is about the same as for $\mathrm{d}\lambda^2/\nu\mathrm{d}t$ for this region, consistent with the suggestion above that the integral scale behaviour is closely linked to the constancy (or lack of it) of n. As noted in Appendix A, the spectra for both sets of data show a remarkable collapse for all wavenumbers (except the lowest one) when normalized with u^2 and λ. This also implies L/λ is constant, since both the integral scale and the Taylor microscale are determined from the spectrum.

https://doi.org/10.1017/S002211200200811X Published online by Cambridge University Press

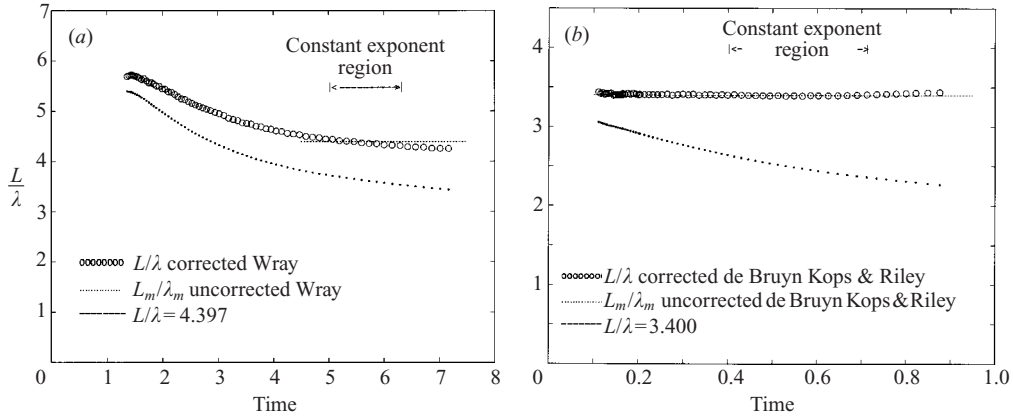


FIGURE 8. Corrected and uncorrected L/λ versus t for (a) Wray (1998) data, (b) de Bruyn Kops & Riley (1998) data.

5. Summary and conclusions

A simple spectral model was used to evaluate the effect of the missing large scales on estimates of the energy and integral scales in homogeneous turbulent flow. The results apply both to experiments (which are limited by the tunnel dimensions) and to DNS data (which are limited by computational box-size or the lowest wavenumber). The fundamental idea is that periodic and box turbulence can be viewed as models of isotropic turbulence in an infinite environment, but with the largest scales simply missing. This has long been implicitly assumed by the turbulence community, but there has been no systematic methodology for examining the differences. The most likely reason for the success of this simple approach is that the largest scales of motion interact only weakly with the rest of the flow since their time scales are very large. Even so, the approximation must break down for very large decay times, unless it can be shown that there would be no flux of energy into wavenumbers below the low-wavenumber cutoff. This might indeed be the case if the cutoff is in the low-wavenumber spectral region believed (at least by some, e.g. George 1992) to be invariant.

For the energy and Taylor microscales, the dependence on the specific behaviour at low wavenumbers is weak as long as the ratio of the lowest wavenumber to the peak wavenumber is less than 0.2. Even a small error, however, creates an apparent time dependence of the decay parameters. For the integral scale, however, the dependence on the specific form of the spectrum near $k = 0$ is quite important, and the limitations on the ratio of lowest wavenumber to peak wavenumber are much more severe. Typically, $k_L/k_p < 0.1$ is necessary to ensure less than 10% error. Almost no experimental or DNS data to date satisfy this criterion except for the earliest decay times. Similar criteria apply to the important ratio of integral to Taylor microscale, which can be substantially reduced during decay by the missing wavenumbers.

It was shown to be possible to correct the estimated integral scales of the approximately isotropic decaying turbulence for the effect of the missing wavenumbers by solving equation (3.5) interatively. Application to two different DNS data sets produced conflicting evidence. The most that can be said is that $L \propto t^{1/2}$ if the energy decays as a power law in time with constant exponent (i.e. $n = constant$), but if $n \neq constant$ (for whatever reason) perhaps it does not. The somewhat slower growth rates reported in the literature as well as their variation are most probably directly

https://doi.org/10.1017/S002211200200811X Published online by Cambridge University Press

related to the missing large scales, exactly as suggested earlier by Comte-Bellot & Corrsin (1971).

Correction of any data is never a satisfying proposition, no matter how carefully performed, since in some sense it presumes the answer. Therefore, it can at most provide tentative conclusions which point the way to further experiments or simulations. Even so, the spectral theory used to correct the data here was quite independent of the similarity analysis, except for the assumed value of p, the exponent describing the behaviour of the spectrum for small k. It can certainly be said that the corrected data were internally consistent with the single-point constraints for isotropic homogeneous turbulence; the relation between the decay exponent and the time derivative of the Taylor microscale squared (equation (4.5)) is most important. This relation does not seem to have been previously applied to other attempts to determine the appropriate energy power law for either simulations or experiments, but it should be in all future efforts.

What is the significance of these results? First, this study makes clear once again that considerable care must be taken before using the results of experiments and DNS to infer the behaviour of isotropic turbulence. A perfect experiment and a perfect simulation is at best an approximation to this ideal state. And even though it may provide an adequate approximation for one statistical quantity, it may not for another. Secondly, the turbulence community as a whole has been all too willing to dismiss the contributions of isotropic turbulence theory and especially similarity theory as being wrong or irrelevant. This study suggests the opposite. When carefully applied, both provide powerful tools for evaluating the limitations of our attempts to study turbulence in the laboratory or by computer.

Neither of the DNS simulations considered herein were optimized for the questions asked here. Therefore, the authors are especially grateful to Dr A. Wray of NASA Ames and Dr S. de Bruyn Kops and Professor J. Riley of the University of Washington for graciously making their data available to us. We would also like to thank S. Gamard of Chalmers for his assistance with the optimizations. The many helpful discussions with T. G. Johansson and C. Wollblad are also gratefully acknowledged.

This work was initiated while the authors were participating in the Hydrodynamic Turbulence Program of the Institute for Theoretical Physics at UCSB in the spring of 2000. Memories of the encouragement and support of the organizers, staff, and participants of that stimulating environment will long be cherished by us both. We are especially grateful to Professor K. Sreenivisan of Yale for the invitation to participate.

Appendix A. Details of the spectral model

The spectral model of equation (3.3) is repeated here for convenience:

$$E(k,t) = u^2 L \frac{C_p (kL)^p}{[1 + (k/k_e)^2]^{p/2+5/6}}. \tag{A 1}$$

The coefficients C_p and k_e (or equivalently L or k_p) are interrelated and can be determined by direct substitution of equation (3.3) into equations (2.1) and (2.2). The resulting normalization integrals for the energy and integral scale are:

$$\tfrac{3}{2} = C_p (k_e L)^{p+1} \int_0^\infty \frac{x^p}{[1 + x^2]^{p/2+5/6}} \mathrm{d}x, \tag{A 2}$$

https://doi.org/10.1017/S002211200200811X Published online by Cambridge University Press

p	1	1.34	2	3	4
k_pL	1.3630	1.2943	1.2272	1.1804	1.1570
k_eL	1.7597	1.4437	1.1203	0.8798	0.7468
k_p/k_e	0.7746	0.8965	1.0954	1.3416	1.5492
C_p	0.3229	0.4535	0.8455	2.2249	6.2528

TABLE 1. Spectral parameters as function of p.

and

$$1 = \tfrac{1}{2}\pi C_p(k_eL)^p \int_0^\infty \frac{x^{p-1}}{[1+x^2]^{p/2+5/6}}\mathrm{d}x. \tag{A 3}$$

By using $t = 1/(1+x^2)$, the integrals can be transformed into the familiar beta function defined by:

$$B(a,b) = \int_0^1 t^{a-1}(1-t)^{b-1}\mathrm{d}t. \tag{A 4}$$

The results are:

$$\tfrac{3}{2} = \tfrac{1}{2}C_p(k_eL)^{p+1}B(\tfrac{1}{3},\tfrac{1}{2}(p+1)), \tag{A 5}$$

and

$$1 = \tfrac{1}{4}\pi C_p(k_eL)^p B(\tfrac{5}{6},\tfrac{1}{2}p) \tag{A 6}$$

The relation between k_e and L is easily determined by dividing equation (A 6) by equation (A 5). The result is:

$$k_eL = \frac{3\pi}{4}\frac{B(\frac{5}{6},\frac{1}{2}p)}{B(\frac{1}{3},\frac{1}{2}(p+1))}. \tag{A 7}$$

Thus, as noted above, k_eL is a constant dependent only on the value chosen for p.

The value of the coefficient C_p can now be determined by substitution of equation (A 7) into either equations (A 5) or (A 6). The result is:

$$C_p = \left[\frac{4}{\pi B(\frac{5}{6},\frac{1}{2}p)}\right]^{1+p}\left[\frac{B(\frac{1}{3},\frac{1}{2}(p+1))}{3}\right]^p. \tag{A 8}$$

Another wavenumber of interest is the wavenumber at which the spectrum $E(k,t)$ has its maximum, say k_p. It is straightforward to show (by setting $\mathrm{d}E/\mathrm{d}k = 0$) that k_p is given by:

$$\frac{k_p}{k_e} = \left[\frac{3p}{5}\right]^{1/2}. \tag{A 9}$$

Using equation (A 7) yields equation (4.1), i.e.

$$k_pL = \frac{3\pi}{4}\left[\frac{3p}{5}\right]^{1/2}\frac{B(\frac{5}{6},\frac{1}{2}p)}{B(\frac{1}{3},\frac{1}{2}(p+1))}. \tag{A 10}$$

Values of k_pL, k_eL, k_p/k_e and C_p are given in table 1 for $p = 1$, 1.34, 2, 3 and 4.

Figure 9 shows the de Bruyn Kops & Riley data plotted together with the model spectrum equation (3.3). Only the data beyond $t \geqslant 0.287$ have been plotted, since this is just before the region of constant power exponent decay begins. The data have been normalized using the corrected values of u^2 and λ discussed in § 4, and the model

https://doi.org/10.1017/S002211200200811X Published online by Cambridge University Press

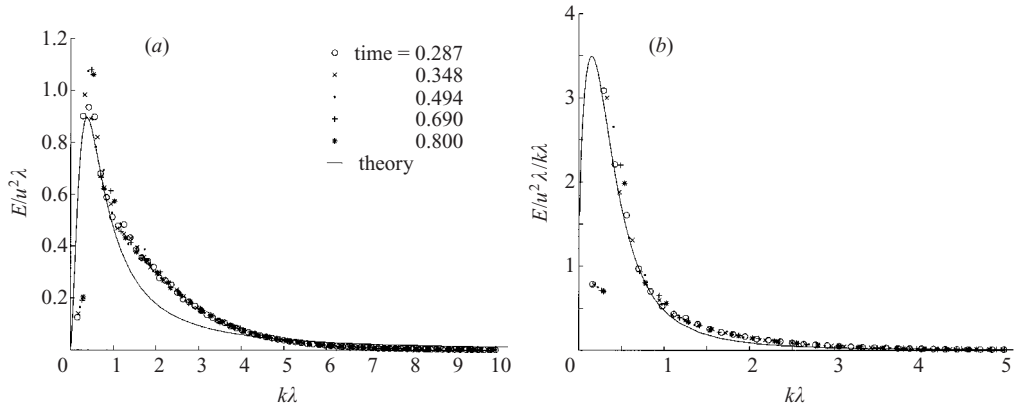


FIGURE 9. (*a*) $E(k)/u^2\lambda$ and (*b*) $E(k)/u^2\lambda/k\lambda$ versus $k\lambda$ for the de Bruyn Kops & Riley (1998) DNS data.

spectrum has been converted to these variables using the constant value of $L/\lambda = 3.4$. The value of $p = 1.34$ was chosen by iteration and by requiring $\mathrm{d}\lambda^2/v\mathrm{d}t = 20/(p+1)$. The model spectrum is in reasonable agreement with the low-wavenumber data for all but the lowest wavenumber. This lowest wavenumber is always problematical for the simulations, since it is at the very edge of the averaging integral. In fact, if p is determined using only the lowest wavenumbers on these plots, it is less than unity, suggesting strongly that the lowest wavenumber estimate is too low.

By contrast, the $k^{-5/3}$ roll-off of the infinite Reynolds number model is a bit too fast for these low Reynolds numbers, exactly as observed by Mydlarski & Warhaft (1996) (see also Gamard & George 2000). Since all plots are normalized to integrate to the same energy, the lack of exponential tail on the model spectrum used here means there must be slightly less energy at low wavenumbers to compensate for the extra energy at high wavenumbers. Even this effect is not evident in the plot of E/k for which both models are in excellent agreement with the data for all but the questionable lowest wavenumber. However, this behaviour is irrelevant to the considerations here, since only the behaviour around and below the spectral peak are important for the correction to the energy and integral scale. Thus, the ratios of u_m^2/u^2 and L_m/L are unaffected.

Figure 10 shows the same plots for the Wray (1998) data. A value of $p = 2$ was determined to provide the best consistency with the $\mathrm{d}\lambda^2/v\mathrm{d}t$ plots, and a constant value of $L/\lambda = 4.4$ was used to convert the model curve to these variables. As noted above, the exponent of the power law decay is at most constant for only the limited range from $5 < t < 6.3$. Nonetheless, the normalization works remarkably well, even though there is only a limited power law region. The spectral fit to the higher wavenumbers is better than for the de Bruyn Kops & Riley data because the Reynolds number of the data is higher. The problem with the lowest wavenumber is also less severe.

Appendix B. Details of partial integrals for u^2 and L using the spectral model

The effect of the missing low wavenumbers on the integrals can be evaluated by substituting the spectral model of equation (3.3) into equations (3.1) and (3.2) to obtain the ratios u_m^2/u^2 and L_m/L directly.

https://doi.org/10.1017/S002211200200811X Published online by Cambridge University Press

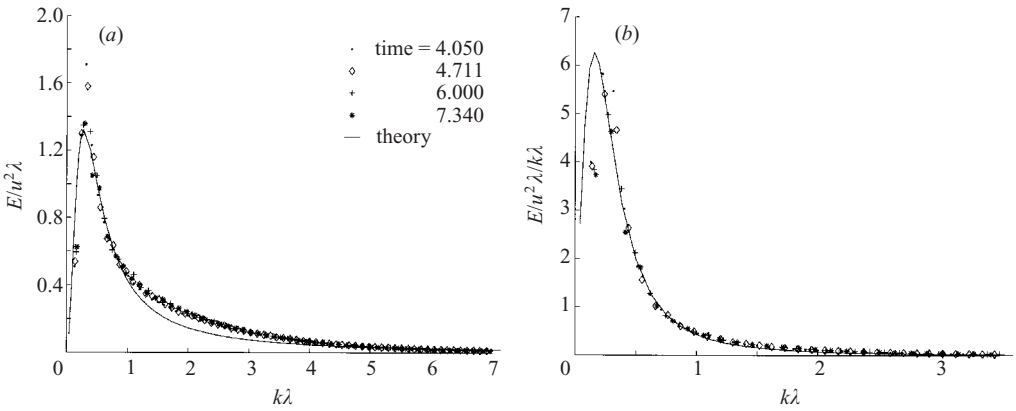


FIGURE 10. (a) $E(k)/u^2\lambda$ and (b) $E(k)/u^2\lambda/k\lambda$ versus $k\lambda$ for the Wray (1998) DNS data.

Again using $t = 1/(1+x^2)$, the integrals can be transformed into the incomplete beta function defined by:

$$I_z(a,b;z) \equiv [B(a,b)]^{-1} \int_0^z t^{a-1}(1-t)^{b-1}\mathrm{d}t. \tag{B 1}$$

Equations (3.4) and (3.5) follow after some manipulation, i.e.

$$\frac{u_m^2}{u^2} = I_z(\tfrac{1}{3}, \tfrac{1}{2}(p+1); z) \tag{B 2}$$

and

$$\frac{L_m}{L} = \frac{u^2}{u_m^2} I_z(\tfrac{5}{6}, \tfrac{1}{2}p; z) = \frac{I_z(\tfrac{5}{6}, \tfrac{1}{2}p; z)}{I_z(\tfrac{1}{3}, \tfrac{1}{2}(p+1); z)}, \tag{B 3}$$

where z is defined by equation (3.6) as before. It is straightforward to express either of these in terms of $k_L L$ using equations (A 7) or (4.1). These results have been plotted in figures 3 and 4 for values of $p = 1, 2, 3$ and 4.

Several of the incomplete beta function integrals reduce to elementary analytical expressions. For example, for $p = 1$, u_m^2/u^2 can be expressed simply as:

$$\frac{u_m^2}{u^2} = \frac{1}{[1 + \frac{3}{5}(k_L/k_p)^2]^{1/3}} \quad (p = 1). \tag{B 4}$$

For $p = 2$, L_m/L reduces to:

$$\frac{L_m}{L} = \frac{u^2}{u_m^2} \frac{1}{[1 + (\frac{6}{5})(k_L/k_p)^2]^{5/6}} \quad (p = 2). \tag{B 5}$$

REFERENCES

BATCHELOR, G. K. 1953 *Homogeneous Turbulence*. Cambridge University Press.

DE BRUYN KOPS, S. M. & RILEY, J. J. 1998 Direct numerical simulation of laboratory experiments in isotropic turbulence. *Phys. Fluids* **10**, 2125–2127.

COMTE-BELLOT, G. & CORRSIN, S. 1966 The use of a contraction to improve the isotropy of grid-generated turbulence. *J. Fluid Mech.* **25**, 657–682.

COMTE-BELLOT, G. & CORRSIN, S. 1971 Simple Eulerian time correlation of full- and narrow-band velocity signals in grid-generated, 'isotropic' turbulence. *J. Fluid Mech.* **48**, 273–337.

https://doi.org/10.1017/S002211200200811X Published online by Cambridge University Press

Deissler, R. G. 1961 Analysis of multipoint-multitime correlations and diffusion in decaying homogeneous turbulence. *NASA Tech. Rep.* R-96.

Dryden, H. L. 1943 A review of the statistical theory of turbulence. *Q. Appl. Maths* **1**, 7–42.

Gamard, S. & George, W. K. 2000 Reynolds number dependence of energy spectra in the overlap region of isotropic turbulence. *J. Flow Turbulence Combust.* **63**, 443–447.

George, W. K. 1992 The decay of homogeneous isotropic turbulence. *Phys. Fluids* A **4**, 1492–1509.

George, W. K., Wang, H, Wollblad, C. & Johansson, T. G. 2001 'Homogeneous turbulence' and its relation to realizable flows. *Proc. 14th Australasian Fluid Mech. Conf. 10–14 December 2001, Adelaide University*, pp. 41–48.

Jimenez, J., Wray, A. A., Saffman, P. G., & Rogallo, R. S. 1993 The structure of intense vorticity in isotropic turbulence. *J. Fluid Mech.* **255**, 65–90.

von Kármán, T. & Howarth, L. 1938 On the statistical theory of turbulence. *Proc. R. Soc.* A **164**, 192–215.

Kolmogorov, A. 1941 The local structure of turbulence in incompressible viscous fluid for very high Reynolds numbers. *C. R. Akad. Sci. SSSR* **30**(4), 299–304.

Lohse, D. 1994 Crossover from high to low Reynolds number turbulence. *Phys. Rev. Lett.* **73**, 12.

Mydlarski, L. & Warhaft, Z. 1996 On the onset of high Reynolds number grid generated wind tunnel turbulence. *J. Fluid Mech.* **320**, 331–368.

Sreenivasan, K. R. 1984 On the scaling of the energy dissipation rate. *Phys. Fluids* **27**, 1048–1051.

Wang, H., Gamard, S., Sonnenmeier, J. R. & George, W. K. 2000 Evaluating DNS of isotropic turbulence using similarity theory. *Proc. ICTAM 2000, Chicago, IL 27 August–1 September 2000.* (Extended version available as a Turbulence Research Laboratory Rep. from http://www.tfd.chalmers.se/trl.)

Wray, A. 1998 Decaying isotropic turbulence. In *AGARD Advisory Rep.* **345**, 63–64.

https://doi.org/10.1017/S002211200200811X Published online by Cambridge University Press